ISBN: 978-3-95450-214-1 ISSN: 2673-5490 doi:10.18429/JACoW-IPAC2021-FRXB02

DEVELOPMENT OF 36 GHz RF SYSTEMS FOR RF LINEARISERS*

A. Castilla† [1,2], J. Cai[1,2], G. Burt[2], Engineering Department, Lancaster University, Lancaster, UK
X. Wu, A. Latina, X. Liu, I. Syratchev, W. Wuensch, CERN, Geneva, Switzerland
L. Zhang, L. J. R. Nix, A. W. Cross, Strathclyde University, Glasgow, UK
B. Spataro, M. Behtouei, INFN-LNF, Rome, Italy
[1]also at CERN, Geneva, Switzerland
[2]also at Cockcroft Institute, Daresbury Laboratory, Warrington, UK

Abstract

As part of the deign studies, the CompactLight project plans to use an injector in the C-band. Which constitutes a particular complication for the harmonic system in charge of linearising the beam's phase space, since it means its operation frequency could be higher than the standard X-band RF technologies. In the present work, we investigated a 36 GHz (Ka-band) as the ideal frequency for the harmonic system. A set of structure designs are presented as candidates for the linearisers, based on different powering schemes and pulse compressor technologies. The comparison is made both in terms of beam dynamics and RF performance. Given the phase stability requirements for the MW class RF sources needed for this system, we performed careful studies of a Gyro-Klystron and a multi-beam klystron as potential RF sources, with both showing up to 3 MW available power using moderate modulator voltages. Alternatives for pulse compression at Ka-band are also discussed in this work.

INTRODUCTION

A next generation hard X-ray Free Electron Laser (FEL) facility, based on state-of-the-art, high-gradient, 12 GHz (X-band) RF cavities has been designed by the E.U. funded CompactLight* project. This machine will start with a full 6 GHz (C-band)injector before an X-band main linac that capitalises on the higher gradients available at higher frequencies. This light source facility will operate up to 1 kHz repetition frequency for the soft X-ray (SX) regime.

Typically, XFELs choose to have long bunches in the injector and to use magnetic compressors to generate short electron bunches (around 1-5 fs), with high bunch charges. An energy chirp along the bunch, before the bunch compressors, is needed in order to have the path lengths through the magnetic chicane to be energy dependant. Thus, compressing the bunches in time. Running the injector off-crest introduces the necessary chirp. However, following the sinusoidal shape of the voltage, the chirp is not linear in time, and for this reason a harmonic system is used to linearise the chirp. After looking into different frequency options, 36 GHz (Ka-band) was found to be an optimal working point.

A high frequency system, like this one, will require relatively small apertures, making the wakefield contribution an important factor. Other issues are derived from the lack of availability of, off the shelve, high power amplifiers at this frequency. And for all these reasons, this paper presents work done in order to achieve a full and feasible RF system, suitable for use as a linearisers. The feasibility of manufacturing Ka band structures and operating them at very high gradients has been established in the context of the CLIC study [1–3].

This paper presents a condensed summary of the work performed by the authors to develop 36 GHz RF systems for FEL applications, a complete version of this work has been recently submitted for publication to a journal [4]. The reader is encouraged to refer to that article for further details.

VOLTAGE REQUIREMENTS

Considering the low average momentum (300 MeV) and relative long bunches at the linearisers's location, the effects of the short-range wakefield define the minimum iris aperture radius (denoted as a, see Fig. 1) for the 36 GHz structure. After careful analysis, the selected working point was fixed at 30 cm for the structure's length, and $a = 2$ mm.

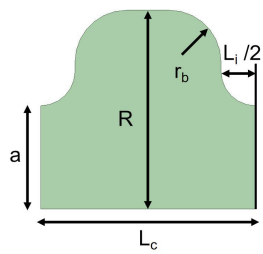

Figure 1: Single cell geometry.

We can only be sure of how well the linearisers is working by looking at the bunch shape at the end of our linac and, ultimately, the photons coming out of the undulators. In that sense, the 36 GHz linearisers must be integrated to the gymnastics of the injector and main linac in order to assess the total RF curvature and the wakefields coming from the RF systems and any non-linear effects generated or amplified by the magnetic chicanes.

Due to the multiple contributions to the nonlinear effects in the longitudinal plane, the only way to fix the optimised voltage needed from the linearisers, is to perform a start-to-end longitudinal optimisation, including all the aforementioned elements. For this work, this optimisation was done using the 1D tracking code "Track1D". The resulting re-

* This project has received funding from the European Union's Horizon2020 research and innovation programme under grant agreement No 777431.
† a.castilla@cern.ch

ISBN: 978-3-95450-214-1 ISSN: 2673-5490 doi:10.18429/JACoW-IPAC2021-FRXB02

quired integrated voltage was fixed at $V_{\mathrm{Ka}} = 12$ MV and Fig. 2 shows an example of start-to-end tracking of the CompactLight accelerator, obtained with the code Track1D [5].

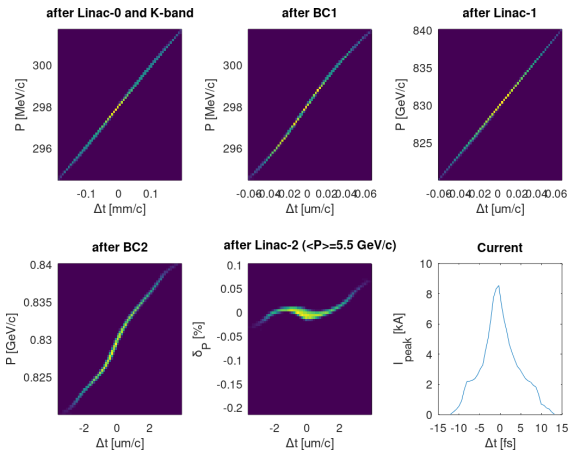

Figure 2: Example of start-to-end tracking, obtained with the code Track1D.

RF SOURCES

The use of klystrons as RF sources is common in almost all large linacs above 1 GHz, since they can generate large peak powers. However, for high frequencies, the gap needed becomes too small to handle high powers, rendering klystrons unpractical. The use of Higher order mode (HOM) cavities is necessary to overcome this issue, as their larger diameter (for a given frequency) improves their performance. Mode separation is an issue in HOM cavities, so an amplifiers that works with this principle needs to excite a single mode only. We present now two options of doing this: a gyro-klystron which uses a rotating beam to interact with a single mode, and a HOM multi-beam klystron (HOM-MBK) that uses multiple beams, in order to cancel out undesired modes.

Gyro-klystron

A gyro-klystron with 3 MW output power was designed as the driving source for the lineariser, using a three-cavity configuration [6, 7]. With the input and intermediate cavities operating in a TE_{01} mode, while the output cavity operates at a higher-order TE_{02} mode to improve the power handling capability. The RF signals to/from the gyro-klystron are coupled by a pillbox microwave window and a single-disk microwave window, respectively.

The interaction circuit for the gyro-klystron was designed as an iterative process. Starting with a small-signal linear theory, based on the point-gap approximation, used to find the constrains of the initial parameters, such as the beam current, voltage, the transverse-to-axial velocity ratio α, and the magnetic field strength at the interaction region [8]. After choosing the core beam parameters, eigenfrequencies, and the cavities' quality factors, then the cavity dimensions are fixed. Then, the gyro-klystron's efficiency was evaluated using the nonlinear simulation model. Since the nonlinear model uses the cavities' field profiles, it can give detailed information on the bunching process, and more accurate gain and interaction efficiency. The nonlinear theory provides a good balance between accuracy and computation time to investigate a large parameter space [9]. Lastly, particle-in-cell (PIC) simulations validate the design obtained from the nonlinear simulation.

Figure 3 shows the geometry of the gyro-klystron cavities and phase space of the electrons in the PIC simulation. The final design parameters are presented in Table 1.

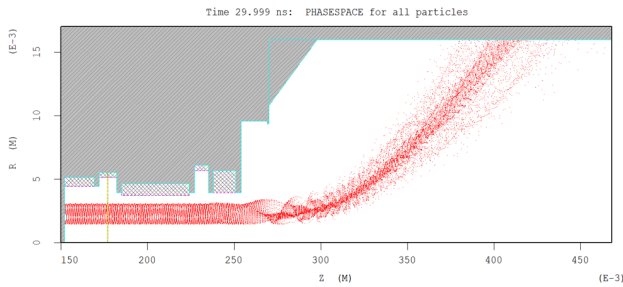

Figure 3: Phase space of the electrons in the gyro-klystron.

Table 1: 36 GHz Gyro-klystron's Initial Parameters

Parameter	Value	Units
Beam voltage V_b	150	kV
Beam current I_b	50	A
Transverse-to-axial velocity ratio α	1.50	–
Magnetic field strength B_0	1.49	T
Bandwidth	190	MHz
Output frequency	36	GHz
Output power	3.2	MW
Efficiency	42	%
Gain	48	dB

A magnetron injection gun (MIG) [10] is used to generate the gyro-klystron's small-orbit gyrating electron beam. A triode-type gun was designed using the parameters given in Table 1, to provide better control of the beam velocity ratio by means of adjusting the modulating anode voltage.

HOM Multi-Beam Klystron

The goal for our design is to generate 2.5 MW of RF power at 36 GHz. To avoid the need of an oil tank and to reduce the amplifier's length, we chose a cathode voltage of 60 kV. The use of 20 beamlets at 6 A each, was selected to reach a 35% efficiency (i.e. total beam current 120 A and 8.33 MW of beam power). The cavity needs to be big enough to fit in the 20 beamlets, while small enough to have good mode separation between the operating and nearby modes. We conclude, then, that a circular ring cavity with a beam tunnel aperture of 2 mm, width = height = 5.9 mm, and the median cavity radius r = 37.6 mm, operating in the $TM_{20,0}$ mode, was the best option. A required field with 3 to 4 times the Brillouin field strength (0.55 T, in our case),

ISBN: 978-3-95450-214-1 ISSN: 2673-5490 doi:10.18429/JACoW-IPAC2021-FRXB02

for a 2 mm aperture, can be generated without the need of a superconducting magnet.

The cavity positions and tunings were optimised in the disk-model KlyC [11], before being verified in the PIC code CST Particle Studio®. The optimised HOM MBK provides 2.5 MW peak power, with 35% efficiency and a 50 MHz (-3 dB) bandwidth, with 40.7 dB gain. Table 2 summarises the operating parameters of the optimised tube.

Table 2: Initial Parameters for the 36 GHz HOM MBK

Parameter	Value	Units
Beam voltage V_b	60	kV
Beam current I_b	120	A
Magnetic field strength B_0	0.55	T
Bandwidth	50	MHz
Output frequency	36	GHz
Output power	2.5	MW
Efficiency	35	%
Gain	40.7	dB

The competition between the operating and nearby modes was studied by means of turning off the individual beamlets one by one. We only saw a reduction of 7% in the RF power, consistent with the 5% contribution of each beamlet to the total current. A small reduction to the efficiency is also observed due to the change of the total perveance. Figure 4 shows the footprint of this amplifier.

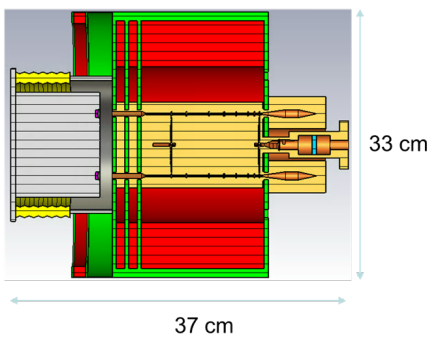

Figure 4: Diagram showing the footprint of the HOM-MBK design.

PULSE COMPRESSOR

Both sources discussed in this paper can provide between 3.2 MW and 2.5 MW of RF peak power at 36 GHz, at up to 1 kHz repetition rate. However, these power levels are unlikely to be sufficient for building up the necessary fields on the linearisers. Luckily, the needed pulse lengths to fill a 36 GHz cavity are well below the 1 µs pulses provided by either of the sources considered here. This allows the use of a pulse compressor to increase the peak power, capitalising from the relatively long RF pulse, hence reducing the needed number of RF amplifiers.

The delay line SLEDII pulse compressor is discussed in detail in [12, 13]. The delay line length of this compressor, is proportional to the output pulse width. It is possible to reduce the total delay line length by a factor of "n", where "n" is the number of modes used simultaneously in the same line, using reflective delay lines that transmit the RF power in several modes [14, 15]. A two moded SLEDII pulse compressor, uses two modes (circular TE01 and TE02) in the same delay line, and hence cutting by a factor of 2 the delay line length.

In the case of CompactLight, a two-bunch operation with 0.83 ns spacing is envisioned. As the spacing is much smaller than the filling time of the lineariser, the needed RF pulse width is dominated by the structure's filling time, allowing for shorter delay line lengths, compared to those used in colliders with need of longer pulses [14].

In the case of a 300 mm traveling wave structure (TWS), operating at a $2\pi/3$ mode, the fill time is 8.4 ns. Hence, a 1.43 m, two moded delay line, that includes the filling time, as well as the rise/fall edge of the RF pulse, can provide power gains of ~697%, given a 510 ns pulse coming from the RF sources, reaching up to 15 MW in a 20 ns compressed pulse. Figure 5 shows the normalised pulse coming from the source (in blue) and the compressed pulse (in red).

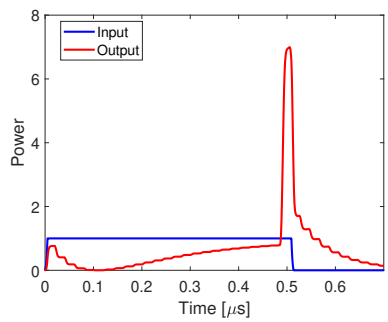

Figure 5: Normalised 510 ns input pulse from the RF source (blue) and 20 ns compressed pulse after the two moded SLEDII pulse compressor (red).

TRAVELLING WAVE STRUCTURE

The 36 GHz, TWS, single cell geometry, was optimised for 3 different phase advances and the general parameters of the 120° case are presented in Table 3 for their comparison.

After careful inspection of the $\phi = 2\pi/3$, $\phi = 5\pi/5$, and $6\pi/7$ phase advances, we concluded that, for our case, having relative large apertures (where $a \approx \lambda/4$), the lower phase advance option is better to provide the target voltage (i.e. 12.75 MV) with lower power requirements for a given structure length (see Fig. 6).

Figure 6 displays the possible combinations of input power and structure length to provide, at least, a linearising voltage of 12.75 MW. The lower border of the colored areas represent the combinations where a minimal input power is needed to provide the required voltage for a certain structure length. The red dashed lines indicate the chosen operating point, where a 300 mm long, $\phi = 2\pi/3$ TWS, provides the 12.75 MV with 15 MW of RF power. From this plot we

ISBN: 978-3-95450-214-1 ISSN: 2673-5490 doi:10.18429/JACoW-IPAC2021-FRXB02

Table 3: TWS Single Cell Parameters

Parameter	Value	Units
Frequency f	36	GHz
Q factor	4392	- -
Shunt impedance r_L	106	MΩ / m
Group velocity v_g	0.119	c
Attenuation α_0	0.7	m^{-1}
Peak surface field E_p^*	2.57	MV/m
Cavity radius R	3.96	mm
Iris radius a	2.00	mm
Cell length L_c	2.78	mm
Iris thickness L_i	0.60	mm

*Normalised to E_{acc} = 1 MV/m.

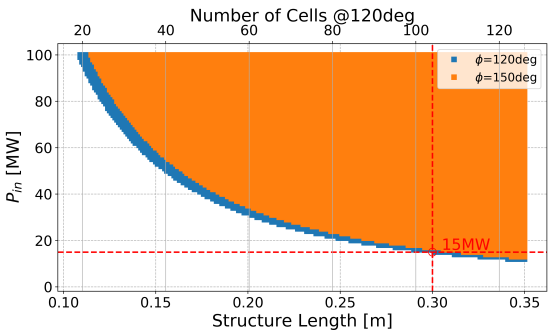

Figure 6: Available power and structure length combinations that provide 12.75 MV integrated voltage, for the 36 GHz at $2\pi/3$ (blue), and $5\pi/6$ (orange) phase advances.

can see that in order to reduce the structure length by one third (i.e. 200 mm), would require to double the required input power. It is perhaps important to notice that, even when shorter structures will require shorter compressed pulses, the compression factor of the pulse compressor saturates at some point, and going to longer rf pulses, or shorted compressed pulses for that matter, does not provide a practical increase of the power gains, rendering a shorter option unpractical.

Therefore, we propose a 108 cells (300 mm), constant impedance, $2\pi/3$, TWS as the linear baseline for the CompactLight project.Such structure is capable of reaching the required 12.75 MV integrated voltage, for the available 15 MW of RF power after compression. The power dissipation of the 36 GHz TWS linear (2.5 kW/m), is comparable to that of the CompactLight main linac (2.4 kW/m), when both are operating at nominal gradient and 1 kHz repetition rate.

STANDING WAVE STRUCTURE

There are two issues with a standing wave cavity. The first one being the availability of 36 GHz MW-class circulators, this can be assessed by the use of structures in pairs and hybrid couplers, to avoid reflections by means of choosing the proper phase delay between structures. The number of structures needed will be higher due to cell-to-cell coupling restrictions in a standing wave structure, and the cells at 36 GHz will be very short. The second problem is the delay line length needed to provide the long compressed pulses. For instance, the 120-150 ns puse needed to fully fill a SWS, requires about 8.5 m long of delay line. However, this can be overcome if we use instead partly filled cavities. Since the instantaneous voltage in SWS fill very quickly at the beginning (following an exponential), and a 50 ns rectangular pulse is sufficient to fill about 85% of the maximum voltage.

If the small 36 GHz structures are found to have problems handling the same power per unit length as the CompactLight main linac, an option with a lower heat load would be needed. Hence, due to their lower average power requirements, the SWS option is kept as an alternative design for CompactLight.

The SWS design is based on either two or four 19-cell standing wave structures. The cell geometry is shown in Fig. 1 and the general parameters are presented in Table 4.

Table 4: SWS Single Cell Parameters

Parameter	Value	Units
Frequency f	36	GHz
Q factor	5941	- -
Shunt impedance r_L	97.7	MΩ / m
Peak surface field E_p^*	2.67	MV/m
Filling time T_{fill}^{**}	121	ns
Cavity radius R	3.86	mm
Iris radius a	2.00	mm
Cell length L_c	4.16	mm
Iris thickness L_i	0.667	mm

*Normalised to E_{acc} = 1 MV/m.
**Time to fill 99% of the the steady state field.

To achieve a lower dissipated power on the SWS option, we have found that a 21 ns, 2.52 MW compressed pulse would be sufficient to reach 12.05 MV of integrated voltage (or 38 MV/m) with four 19-cell cavities. Such a compressed pulse can be obtained using a 156 ns pulse from the RF source and a 1.50 m long SLEDII pulse compressor, filling the SWS up to 68% of the voltage at steady state. Resulting in 1.06 kW/m of average dissipated power. However, it is noted that the complication of needing three hybrids as part of the system, to avoid reflections to the amplifiers, remains.

SMALL APERTURE HIGH-GRADIENT OPTION

For applications on which the wakefields constraints are more relaxed than the case discussed so far in this paper, designs with smaller apertures could run at considerable higher gradients. When pushing the envelope of the technology used in future machines, we take on the compromise between beam dynamics, RF parameters, reduced energy spreads, manufacturing tolerances, etc. To reduce the required input power, for a given gradient, the RF structures should be designed to maximise their shunt impedance. We

ISBN: 978-3-95450-214-1 ISSN: 2673-5490 doi:10.18429/JACoW-IPAC2021-FRXB02

discuss now the design of an ultra compact (80 mm) 36 GHz SWS π-mode lineariser, with accelerating gradients beyond 100 MV/m, while keeping low surface fields, reducing breakdowns during operation [16–19].

A design with $a/\lambda = 0.12$ (or $a = 1$ mm) was chosen as an optimal compromise between the RF and beam dynamics performances [19]. Table 5 shows some of the main cavity parameters for this design.

Table 5: Small Aperture 36 GHz SWS Parameter List

Parameter	Value	Units
Frequency	35.982	GHz
Operating Mode	π	–
Peak surface field E_p^*	1.55	MV/m
Peak surface field B_p^*	2.70	mT
Shunt impedance r_L	188	MΩ/m
Unloaded quality factor Q	5628	–
Structure length	80	mm
Iris radius a/λ ratio	0.12	–
Iris thickness L_i	0.667	mm
Ellipse semi-axes iris ratio shape	5/7	–
Cavity radius R	3.628	mm

*Normalised to $E_{acc} = 1$ MV/m.

The modified Poynting S_c and the pulse heating (PH) were carefully studied and found to be within the operation safety thresholds [20–22]. Considering an RF source plus a pulse compressor, similar to scheme the described previously in this paper, we expect to be able to reach 12 MW of input power. A pair of structures and a hybrid should suffice to avoid reflections back to the amplifier. In the case of an 80 mm long $2\pi/3$ mode TWS lineariser, with 1 mm aperture, and 24 MW input power, it is possible to achieve gradients of 125 MV/m, despite its strong attenuation (2.51 m^{-1}).

CRYO-COOLED CU-STRUCTURES

Experiments on S and X-band structures conclusively suggest that the use of cryogenic cooled structures can further reduce the RF power dissipation and the structure's breakdown rates. The scaling of the anomalous skin effect (ASE) [23], and an RF breakdown rate of 2×10^{-4} /pulse/m at 250 MV/m accelerating gradient (500 MV/m peak surface electric field), have been verified for a 150 ns RF pulse in the X-band [24]. Even when the advantage of the dissipation effects is reduced at high frequencies, it is still significant at 36 GHz. High frequency linearisers are critical for applications like the MaRIE XFEL [25], the CompactLight FEL, and the Ultra-Compact XFEL at UCLA [26]. Taking into account the developments of MW-class RF sources at 36 GHz, the design of a compact, high gradient cryogenic lineariser in this frequency range seems feasible [19].

For an optimised 36 GHz structure, at room temperature, the shunt impedance is 158 MΩ/m. Extrapolating the ASE enhancement at cryogenic temperatures from an S-band structure to the Ka-band case, and noting that, for the ohmnic surface resistivity: $R_{s,\Omega} \propto \omega^{1/2}$, while for ASE at low temperatures: $R_{s,ASE} \propto \omega^{2/3}$. We expect and increase in the quality factor of $Q_{enh} \propto \omega^{-1/6}$. For liquid Nitrogen temperatures (77 K) we predict $Q_{enh,77K} \simeq 2.2$, while by going below 40 K we expect up to $Q_{enh,40K} \simeq 3.3$.

As an example, let's assume 5 MW matched input power going into a 77 K, 100 mm structure, with estimated shunt impedance of 349 MΩ/m. The achieved accelerating field is 130 MV/m, which is well below the breakdown limit. The corresponding surface field of 260 MV/m is also below the emission threshold for dark-current beam loading [27].

Figure 7 shows the comparison of the integrated voltages, as function of the matched input power, obtained with a π mode, small aperture ($a = 1$ mm, and $r_1 = r_2 = 5/7$ ellipse semi-axes ratio) SWS, operated both at room (in red) and cryogenic (in blue) temperatures. We can see then, that for the cryogenic case, a single structure with 8 MW input power can provide an integrated voltage of about 15 MV.

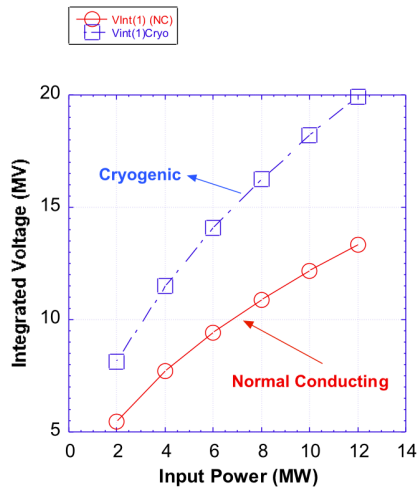

Figure 7: Integrated voltage as function of the input power.

CONCLUSION

A 30 cm long, constant impedance TWS is presented as a baseline option for the CompactLight project, delivering more than 12 MV of linearising voltage at 1 kHz repetition rate, and operating at a gradient of 42.5 MV/m. An option of a two sets of pairs of 19-cells standing wave structures, partially filled (to ~68%) is kept as an alternative option, in case the dissipated power on the TWS is deemed unpractical. The alternatives of compact, higher gradient, and cryogenic operated Cu-structures are kept, in case of insufficient power availability to support the baseline option.

Two RF power sources are developed, each capable of delivering at least 2.5 MW, 1 µs pulses at 1kHz: A HOM MBK that operates with a low cathode voltage, and hence does not requires an oil tank. And a gyro-klystron with even larger saturated peak power. In the case of CompactLight, we are seeking commercial partners for the manufacturing of either of such amplifiers.

ISBN: 978-3-95450-214-1 ISSN: 2673-5490 doi:10.18429/JACoW-IPAC2021-FRXB02

REFERENCES

[1] W. Wuensch, "CLIC 30 GHZ Accelerating Structure Development", CERN, Geneva, Switzerland, Rep. CERN-PS-2002-059-RF, Sep. 2002.

[2] H. H. Braun *et al.*, "Status of CLIC High-gradient Studies", CERN, Geneva, Switzerland, Rep. CERN-PS-2001-045-RF, Jul. 2001.

[3] W. Wuensch *et al.*, "30 GHz Power Production in CTF3", CERN, Geneva, Switzerland, Rep. CERN-AB-2005-030, Jun. 2005.

[4] A. Castilla *et al.*, "Studies of a ka-band lineariser for a compact light source", submitted for publication.

[5] A. Latina, The 1D tracking code, Track1D, https://gitlab.cern.ch/XLS-Git/WP6/-/tree/master/simulation_codes/beam_dynamics/.

[6] L. Wang *et al.*, "Design of a ka-band mw-level high efficiency gyroklystron for accelerators", *IET Microwaves, Antennas & Propagation*, vol. 12, no. 11, pp. 1752–1757, Sep. 2018. doi:10.1049/iet-map.2018.0103

[7] L. J. R. Nix *et al.*, "Demonstration of efficient beam-wave interaction for a mw-level 48 GHz gyroklystron amplifier", *Physics of Plasmas*, vol. 27, no. 5, p. 053 101, 2020. doi:10.1063/1.5144590

[8] G. S. Nusinovich, B. G. Danly, and B. Levush, "Gain and bandwidth in stagger-tuned gyroklystrons", *Physics of Plasmas*, vol. 4, no. 2, pp. 469–478, 1997. doi:10.1063/1.872115

[9] T. M. Tran, B. G. Danly, K. E. Kreischer, J. B. Schutkeker, and R. J. Temkin, "Optimization of gyroklystron efficiency", *The Physics of Fluids*, vol. 29, no. 4, pp. 1274–1281, 1986. doi:10.1063/1.865876

[10] W. Jiang, Y. Luo, R. Yan, and S. Wang, "Genetic algorithm-based shape optimization of modulating anode for magnetron injection gun with low velocity spread", *IEEE Transactions on Electron Devices*, vol. 62, no. 8, pp. 2657–2662, 2015. doi:10.1109/TED.2015.2443068

[11] J. Cai, I. Syratchev, and Z. Liu, "Klyc: Large signal simulation code for klystrons", submitted for publication.

[12] P. B. Wilson, Z. D. Farkas, and R. D. Ruth, "Sled II: A new method of rf pulse compression", in *Proc. 1990 Linear Accelerator Conf. (LINAC'90)*, Albuquerque, NM, USA, Sep. 1990, paper MO456, pp. 204–206.

[13] S. G. Tantawi, R. J. Loewen, C. D. Nantista, and A. E. Vlieks, "The generation of 400-mw rf pulses at x-band using resonant delay lines", *IEEE Transactions on Microwave Theory and Techniques*, vol. 47, no. 12, pp. 2539–2546, 1999. doi:10.1109/22.809004

[14] S. G. Tantawi, "Multimoded reflective delay lines and their application to resonant delay line rf pulse compression systems", *Physical Review Special Topics - Accelerators and Beams*, vol. 7, p. 032 001, Mar. 2004. doi:10.1103/PhysRevSTAB.7.032001

[15] S. G. Tantawi *et al.*, "High-power multimode *X*-band rf pulse compression system for future linear colliders", *Physical Review Special Topics - Accelerators and Beams*, vol. 8, p. 042 002, Apr. 2005. doi:10.1103/PhysRevSTAB.8.042002

[16] B. Spataro and M. Behtouei, "A k band tw accelerating structure for the compact light xls project", presented at WP3 Status Reports, Zurich, Switzerland, Jun. 2018, unpublished.

[17] B. Spataro, "A possible linearizer at 35.982 GHz for the Compact Light XLS project", presented at WP3 Status Report, Zurich, Switzerland, Dec. 2018, unpublished.

[18] M. Behtouei, L. Faillace, M. Ferrario, B. Spataro, and A. Variola, "A ka-band linearizer tw accelerating structure for the compact light xls project", in *Proc. 4th European Advanced Accelerator Concepts Workshop*, Isola d'Elba, Italy, Sep. 2020, p. 012 021. doi:10.1088/1742-6596/1596/1/012021

[19] M. Behtouei, L. Faillace, B. Spataro, A. Variola, and M. Migliorati, "A sw ka-band linearizer structure with minimum surface electric field for the compact light xls project", *Nuclear Instruments and Methods in Physics Research Section A: Accelerators, Spectrometers, Detectors and Associated Equipment*, vol. 984, p. 164 653, 2020. doi:10.1016/j.nima.2020.164653

[20] K. N. Sjobak, A. Grudiev, and E. Adli, "New criterion for shape optimization of normal-conducting accelerator cells for high-gradient applications", in *Proc. 27th Linear Accelerator Conf. (LINAC'14)*, Geneva, Switzerland, Aug. 2014, paper MOPP028, pp. 114–116.

[21] A. Grudiev, S. Calatroni, and W. Wuensch, "New local field quantity describing the high gradient limit of accelerating structures", *Physical Review Special Topics-Accelerators and Beams*, vol. 12, no. 10, p. 102 001, 2009. doi:10.1103/physrevstab.12.102001

[22] D. P. Pritzkau, "Rf pulsed heating", Stanford Linear Accelerator Center, Menlo Park, CA, USA, Rep. SLAC-R-577, Jan. 2002.

[23] G. Reuter and E. Sondheimer, "The theory of the anomalous skin effect in metals", *Proceedings of the Royal Society of London. Series A. Mathematical and Physical Sciences*, vol. 195, no. 1042, pp. 336–364, 1948. doi:10.1098/rspa.1948.0123

[24] A. Cahill, J. Rosenzweig, V. A. Dolgashev, S. G. Tantawi, and S. Weathersby, "High gradient experiments with x-band cryogenic copper accelerating cavities", *Physical Review Accelerators and Beams*, vol. 21, no. 10, p. 102 002, 2018. doi:10.1103/physrevaccelbeams.21.102002

[25] B. E. Carlsten, P. M. Anisimov, C. W. Barnes, Q. R. Marksteiner, R. R. Robles, and N. Yampolsky, "High-brightness beam technology development for a future dynamic mesoscale materials science capability", *Instruments*, vol. 3, no. 4, p. 52, 2019. doi:10.3390/instruments3040052

[26] J. Rosenzweig *et al.*, "An ultra-compact x-ray free-electron laser", *New Journal of Physics*, vol. 22, no. 9, p. 093 067, 2020. doi:10.1088/1367-2630/abb16c

[27] A. Cahill, J. Rosenzweig, V. Dolgashev, Z. Li, S. Tantawi, and S. Weathersby, "Rf losses in a high gradient cryogenic copper cavity", *Physical Review Accelerators and Beams*, vol. 21, no. 6, p. 061 301, 2018. doi:10.1103/physrevaccelbeams.21.061301